Narrow depression in the density of states at the Dirac point in disordered graphene

L. Schweitzer
Physikalisch-Technische Bundesanstalt (PTB), Bundesallee 100, 38116 Braunschweig, Germany
(Received 22 July 2009; revised manuscript received 12 November 2009; published 21 December 2009)

The electronic properties of noninteracting particles moving on a two-dimensional bricklayer lattice are investigated numerically. In particular, the influence of disorder in form of a spatially varying random magnetic flux is studied. In addition, a strong perpendicular constant magnetic field B is considered. The density of states $\rho(E)$ goes to zero for $E \to 0$ as in the ordered system but with a much steeper slope. This happens for both cases: at the Dirac point for $B=0$ and at the center of the central Landau band for finite B. Close to the Dirac point, the dependence of $\rho(E)$ on the system size, on the disorder strength, and on the constant magnetic flux density is analyzed and fitted to an analytical expression proposed previously in connection with the thermal quantum-Hall effect. Additional short-range on-site disorder completely replenishes the indentation in the density of states at the Dirac point.

DOI: 10.1103/PhysRevB.80.245430 PACS number(s): 73.23.−b, 71.30.+h, 73.22.−f

I. INTRODUCTION

Despite enormous efforts in recent years, the electronic properties of graphene near the neutrality point that separates conduction and valence bands are still under intense investigations. Theories aimed at describing graphene via a Dirac-type equation have elucidated many intriguing effects such as the physics of massless relativistic particles and Klein tunneling,[1–5] which has been experimentally observed recently.[6,7] The Dirac-fermion approach, which represents an approximation to the true lattice situation, is believed to be valid especially close to energy zero, the so-called Dirac points, where the conduction and valence bands touch each other and the dispersion is linear. Furthermore, nearest-neighbor tight-binding descriptions,[8–10] which particularly emphasize the hexagonal lattice structure of the carbon sheet, have proven to be extremely helpful in understanding the basic transport properties of this promising new material.

Based on the observation of a peculiar quantum-Hall effect,[11–13] it is generally accepted by now that some kind of disorder must be present in the experimental setup. The disorder influences the charge transport through the graphene sheet and affects the measurable quantities at least quantitatively.[14] Yet, which type of disorder is encountered in real samples is still completely unclear or only partly known in some special cases. This lack of knowledge is particularly unfortunate as the definite type of disorder entirely determines the physical properties,[15–21] e.g., leading to complete Anderson localization in the case of short-range electrostatic scattering potentials via chiral symmetry breaking and scattering between valleys.[22,23] For disordered systems, even the single-particle density of states (DOS) near the Dirac point remains still under debate. Depending on the disorder type and approach, a vanishing, a finite, or an infinite DOS at the Dirac point has been suggested for graphene or related models.[24–34]

Also, the interpretation of experimental results is hampered by the uncertainty regarding the precise form of the DOS. Recently, following earlier experimental investigations of the Landau-level splitting in high magnetic fields,[35,36] the opening of a spin (Zeeman) gap in the density of states at the Dirac point has been suggested in the interpretation of magnetotransport measurements on graphene sheets.[37] Only if a gap, separating electron and hole states at the Dirac point, was assumed, the experimental data could be accounted for. Another unexplained experimental observation to be found near the Dirac point in the presence of a strong magnetic field is the divergent resistance,[38,39] which has been attracting considerable attention lately.

Theoretically, the opening of a mobility gap within the central Landau band has been recently discovered by means of detailed two-terminal conductance calculations.[18] It was found that with increasing disorder, the critical energies where the plateau transitions of the Hall conductivity take place, move apart. This splitting of the central conductance peak unveiled the existence of an extra chiral quantum-phase transition occurring at zero energy with critical properties that differ from those of the quantum-Hall transitions.[18]

In the present work, the single-particle density of states is calculated numerically for the same bricklayer lattice model. The presumed ripple disorder is modeled by a spatially varying random magnetic flux with zero mean, pointing perpendicular to the two-dimensional lattice. Also, an additional constant magnetic field is applied that leads to the formation of Landau bands. It is shown that in the disordered case, the density of states goes to zero at the Dirac point not only in the absence of a perpendicular magnetic field. Rather, a narrow suppression in the DOS is obtained also in the presence of a finite magnetic field within the lowest (central) Landau band. This unexpected feature depends essentially on the disorder strength, on the system size, and on the strength of the perpendicular constant magnetic field. Due to the neglect of electron spin in the model Hamiltonian, this outcome cannot be attributed to a Zeeman splitting but must originate from chirality and a disorder-induced interaction between the two sublattices. This consideration is confirmed by the observation that the addition of short-range potential disorder completely destroys the DOS depression near the Dirac point.

II. BRICKLAYER MODEL

In the present study, the two-dimensional honeycomb lattice responsible for the peculiar electronic properties of

graphene is replaced by a bricklayer model[8,9,18] which shares the same topology as the hexagonal lattice. The bricklayer lattice is bipartite and consists of two sublattices that can be constructed by rectangular unit cells of size $2a \times a$ placed along the x direction. The unit cell contains two sites connected by a bond of length a. Each site on one sublattice is attached to three neighbors belonging to the other sublattice by two bonds in the $\pm x$ direction and one alternating bond in the $\pm y$ direction.

A tight-binding Hamiltonian for noninteracting particles with nearest-neighbor transfer energy V in the presence of perpendicular magnetic fields is defined by

$$\mathcal{H}/V = \sum_{x,y}{}' (e^{i\theta_{x,y+a;x,y}} c^{\dagger}_{x,y} c_{x,y+a} + e^{-i\theta_{x,y-a;x,y}} c^{\dagger}_{x,y} c_{x,y-a}) + \sum_{x,y} (c^{\dagger}_{x,y} c_{x+a,y} + c^{\dagger}_{x,y} c_{x-a,y}), \quad (1)$$

where $c^{\dagger}_{x,y}$ and $c_{x,y}$ are creation and annihilation operators of a particle at site (x,y), respectively. The prime at the first sum in Eq. (1) indicates that only transfers along the nonzero vertical bonds are included. The second sum describes the movement in the horizontal chains. The phases, which are chosen to be only associated with the vertical bonds in the y direction

$$\theta_{x,y;x,y+a} = \theta_{x+2a,y;x+2a,y+a} - \frac{2\pi e}{h}\Phi_{x,y} \quad (2)$$

are defined by the total magnetic flux $\Phi_{x,y} = p/q(h/e) + \phi_{x,y}$ threading a given plaquette with upper left corner at site (x,y). The constant magnetic field is given by the fraction p/q of a flux quantum h/e with mutually prime integers p and q so that the tight-binding band splits exactly into $2q$ subbands, and $\phi_{x,y}$ is the random flux part. The latter incorporates the effect of inhomogeneous magnetic fields and mimics the disorder due to corrugations and ripples[40–42] present in real graphene sheets. In contrast to diagonal disorder, it preserves the chiral symmetry and ensures a finite conductivity at the Dirac point.

The random fluxes are drawn from a box distribution $-f/2 \leq \phi_{x,y} \leq f/2$ with zero mean and disorder strength $0 \leq f/(h/e) \leq 1$. Periodic-boundary conditions are applied in both directions to avoid edge and corner effects and the system size was chosen to be commensurate with the spatially constant magnetic field. The eigenvalues $E_i(n)$ of the Hamiltonian (1) were obtained by direct diagonalization of the N_r disorder realizations and used for the calculation of the ensemble averaged density of states $\rho(E)$ within an energy interval ΔE

$$\rho(E)\Delta E = \frac{1}{N_r}\sum_{n=1}^{N_r} \frac{1}{L_x L_y} \int_{E}^{E+\Delta E} \sum_i \delta[E' - E_i(n)] dE'. \quad (3)$$

III. DENSITY OF STATES

A. Magnetic field $B=0$

Starting with the case where the constant part of the magnetic-flux density is zero and only the random-disorder part is present, the ensemble averaged density of states for bricklayer systems of size $L_x \times L_y = 64 \times 128a^2$ is shown in Fig. 1 for different disorder strengths f. With increasing f, the sharp van Hove singularities at $E/V = \pm 1.0$ get rounded and finally disappear. In the same way, the fluctuations, which can be seen for the smallest disorder $f/(h/e) = 0.05$, vanish. The latter are due to finite size effects. Based on an energy resolution of 0.02V as used in Fig. 1, the other curves do neither depend on the shape of the system nor on the size which has been checked within the range $32 \leq L/a \leq 192$. The main consequence of the increasing disorder is seemingly the filling of the valley in the density of states with a strong increase at the Dirac point $E/V = 0$. However, a closer inspection of the energy range near the Dirac point reveals a completely different behavior. As shown in Fig. 2, independent of disorder strength, the DOS always goes down to zero at $E/V = 0$. For small random-flux disorder, the DOS vanishes with a slope that finally becomes $2/(9\pi V^2 a^2)$ in the clean limit. With increasing disorder strength f, this slope becomes steeper and steeper. Since $f/(h/e) = 1.0$ is the strongest random-flux disorder possible, there will always be an energy region around the Dirac point where the density of states goes to zero at $E/V = 0$.

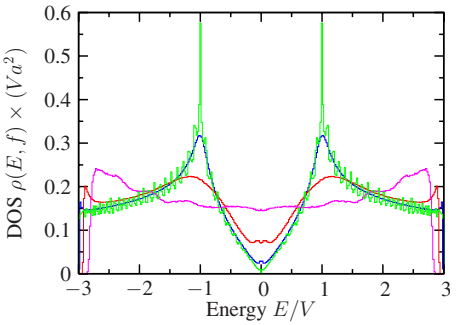

FIG. 1. (Color online) The ensemble averaged density of states of a two-dimensional bricklayer lattice with random-flux-disorder strength $f/(h/e) = 0.05$, 0.2, 0.5, and 1.0. With increasing f, the van Hove singularities disappear. The size of the bricklayer system is $L_x \times L_y = 64 \times 128a^2$.

These results have been obtained with different diagonalization methods including a Lanczos algorithm as well as

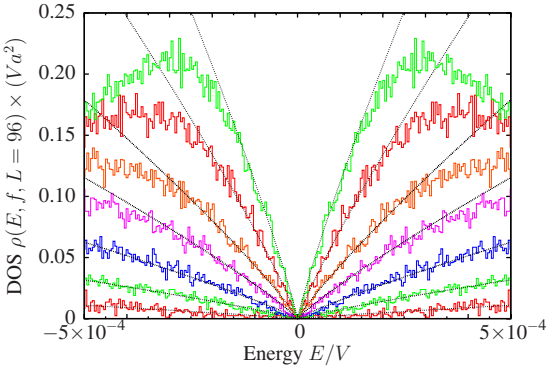

FIG. 2. (Color online) The energy dependence of the density of states near the Dirac point with random-flux disorder strength $f/(h/e) = 0.2$, 0.3, 0.4, 0.5, 0.6, 0.75, and 1.0. The steepest DOS tails belong to $f/(h/e) = 1.0$. The system size is $L_x/a = L_y/a = 96$.

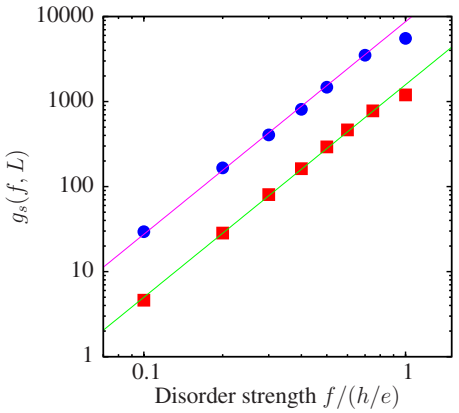

FIG. 3. (Color online) The disorder dependence of the fitting parameter $g_s(f,L)$ with $L/a=96$ for $f/(h/e)=0.1$ and the seven disorder values f shown in Fig. 2. On this double-log plot the straight line is given by $g_s(f)=1580f^{2.5}$. In addition, data for $L/a=192$ (●) are shown with a power-law fit $g_s(f)=8702f^{2.5}$.

standard LAPACK routines. The number of realizations exceeded 10^4 for each disorder f and the DOS bin width $\Delta E/V$ was 4×10^{-6}.

A disorder dependent vanishing of the density of states was previously reported for massless random Dirac fermions on a two-dimensional square lattice[43] and on a honeycomb lattice,[24] where nondiagonal disorder was introduced by real random-hopping terms. These model systems preserve time-reversal symmetry and therefore belong to the (chiral) orthogonal universality class. Also, the energy range where the DOS drops to zero is considerably broader compared with what has been found in our random-flux bricklayer model, which belongs to the chiral unitary symmetry class. Furthermore, the singular peak observed at $E=0$ in Ref. 34 for both the disordered random fermions with either random-hopping or random-gauge fields is absent in the present bricklayer situation.

As seen from the thin black lines used to fit the curves in Fig. 2, neither a simple linear-energy dependence, as observed in the clean system, nor a power-law form used in Refs. 24, 34, and 43 is adequate. An additional logarithmic term similar as in the case of the class D thermal quantum-Hall effect[44,45] or for Dirac fermions on a honeycomb lattice with weak diagonal and bond disorder[24] seems to be an appropriate empirical function. Although bond and random-flux disorder are different, both disorder types maintain the chiral symmetry of the system. Therefore, we try to use the ansatz

$$\rho(E,f,L)=\frac{|E/V|}{2\pi Va^2}\left[1+\frac{2}{\pi}g_s(f,L)\ln\frac{1}{|E/V|}\right] \tag{4}$$

with a disorder and size-dependent fitting function $g_s(f,L)$. The latter grows with both increasing disorder strength and system size L. For square samples of fixed size $L=(96a)^2$ as used in Fig. 2, a power-law dependence on the disorder strength $g_s(f,L/a=96)\propto f^{2.5}$ is found in the range $0.1\le f/(h/e)<1.0$ as is shown in Fig. 3. The same behavior is obtained for larger sizes $L/a=128$ and 192. The latter data are also included in Fig. 3.

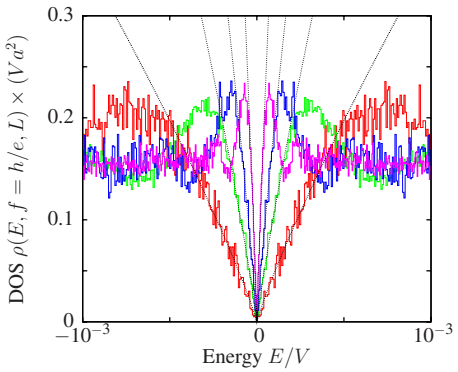

FIG. 4. (Color online) The energy dependence of the density of states for disorder $f=h/e$ and system size $L/a=64$, 96, 128, and 192. With increasing size, the energy range of the DOS depression becomes narrower.

The overall shape of the density of states, as plotted in Fig. 1, seems to be independent of the system size with the exception of noticeable small finite-size fluctuations occurring only for the smallest disorder. In striking contrast, the depression of the DOS near $E/V=0$ shows a strong length dependence. In Fig. 4 the averaged density of states for disorder $f=h/e$ is plotted for sample sizes $L/a=64$, 96, 128, and 192. Applying the function in Eq. (4), the size dependence of g_s close to $E/V=0$ can be obtained. This is shown in Fig. 5 where the size dependence of the fitting parameter $g_s(f,L)$ with $64\le L/a\le512$ is shown on a double-log plot for two disorder strengths $f=1.0$ and $f=0.5$, respectively. In both cases, a power-law relation $g_s(f,L)\propto L^\kappa$ is obtained with an exponent $\kappa=2.0$ for $f=1.0h/e$ and $\kappa=2.15$ if $f=0.5h/e$. Because of the uncertainties due to the limited number of realizations, particularly for larger system sizes, and the restricted range $64\le L/a\le512$, it is not possible to rule out that both exponents are the same in the limit $L\to\infty$. The energy range where the function, Eq. (4), can be fitted to the numerical curves decreases with increasing size L in a similar manner as with increasing disorder strength f, which can be seen in Fig. 2.

With the disorder and size dependence as identified above from the numerical data, our ansatz for the density of states,

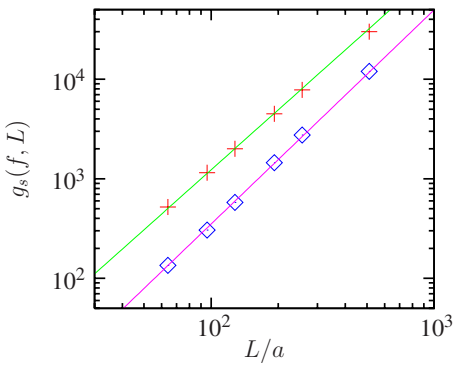

FIG. 5. (Color online) The size dependence of the fitting parameter $g_s(f,L)$ for square samples and two disorder values $f=1.0h/e$ (+) and $f=0.5h/e$ (◇). On a double-log scale, the straight lines are given by $g_s[f/(h/e)=1.0,L]=0.123(L/a)^2$ and $g_s[f/(h/e)=0.5,L]=0.0176(L/a)^{2.15}$, respectively.

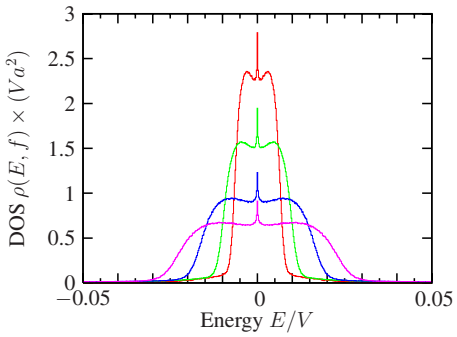

FIG. 6. (Color online) The disorder broadening of the lowest (central) Landau band for square samples of size $L_x=L_y=128a$ and constant magnetic-flux density $p/q=1/32(h/e)a^{-2}$. The disorder strength is $f/(h/e)=0.02$, 0.03, 0.05, and 0.07, respectively.

Eq. (4), used for all curves shown in Fig. 2, is the fitting function $g_s(f,L)=g_c[f/(h/e)]^{5/2}(L/a)^2$ with only one adjustable constant $g_c=0.0925$.

B. Finite magnetic field

For a continuum Dirac model in the presence of a finite magnetic field, the energy spectrum of the charge carriers is arranged into degenerate Landau levels. The energetically lowest Landau level appears at the charge neutrality point at $E=0$.[46] Hence, instead of the density of states going to zero, a finite DOS arises at the Dirac point in the disorder-free system for $B\neq 0$. To account for an external perpendicular B field in our lattice model, a spatially constant magnetic flux is applied in addition to the random-magnetic-flux disorder. This type of disorder causes the central Landau level at the Dirac point to broaden only a little[18,21] compared with the broadening of the higher Landau bands. However, one has to keep in mind that due to the lattice structure, the subbands exhibit Harper's broadening already in the disorder-free system. This intrinsic broadening is small and disappears with decreasing magnetic field. The disorder broadening of the narrow central Landau band, which is proportional to $f\sqrt{p/q}$, is seen in Fig. 6 for $p/q=1/32$ and $L_x=L_y=128a$. There is also an additional narrow structure discernible around $E=0$ and this was previously attributed to originate from the chiral critical eigenstates.[18]

In order to scrutinize this special feature, more than 10^4 disorder realizations were calculated. Thereby, a bin width of about 5×10^{-7} becomes possible leading to an enhanced energy resolution. As a result of this effort, one can see that the density of states in the center of the lowest Landau band is by no means constant but is in fact dominated by a narrow depression (see Fig. 7), which depends on disorder strength, on the constant part of the magnetic flux density, and on the system size. This is an unexpected outcome and was not identified in previous work. It would be very interesting to see whether or not a similar depression with a density of states going to zero at the Dirac point develops also in a continuum Dirac equation approach. The latter method is generally employed in graphene studies and believed to be particularly suited near the Dirac point.

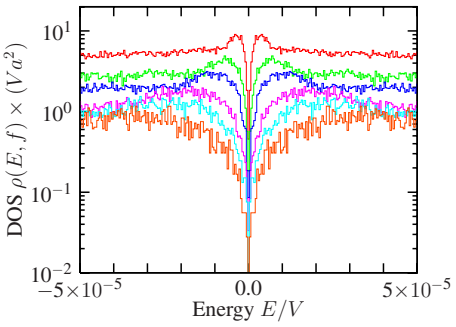

FIG. 7. (Color online) The depression of the density of states within the central Landau band near energy $E/V=0.0$ for square samples of size $L_x=L_y=128a$ and constant magnetic-flux density $p/q=1/32(h/e)a^{-2}$. To enhance the differences, the DOS is shown on a logarithmic scale. The disorder strength for the various curves is $f/(h/e)=0.01$, 0.02, 0.03, 0.05, 0.07, and 0.1, respectively. The topmost curve belongs to $f/(h/e)=0.01$.

The density of states within a narrow energy range near $E/V=0$ is shown in Fig. 7 for square samples of size $L/a=128$, magnetic-flux density $B=1/32(h/e)a^{-2}$ and several disorder strengths f. Contrary to the zero magnetic field case, the tails flatten with increasing disorder for finite B, and the energy range of the DOS depression gets broader. Please note that the DOS is plotted on a logarithmic scale for sake of clarity. A similar function as Eq. (4) can be used to fit the energy dependence of the narrow DOS depression but now with a fitting parameter $g_b(f,L,B)$ which also depends on the constant magnetic-flux density. A power-law relation $g_b(f,L,B)\propto f^{-2}$ is obtained from the data shown in Fig. 7. This behavior is plotted in Fig. 8 for disorder values in the range $0.01\leq f/(h/e)\leq 0.1$. The same dependence has been found also for size $L/a=192$, magnetic flux $p/q=1/96$ and disorder strengths $f/(h/e)=0.01$, 0.02, and 0.05. Therefore, the energy range of the DOS depression broadens with increasing disorder strength and the tails become flat, which is completely opposite to the $B=0$ case.

The specific magnetic field dependence of $g_b(f,L,B)$ is not so easy to extract because both the height and the width

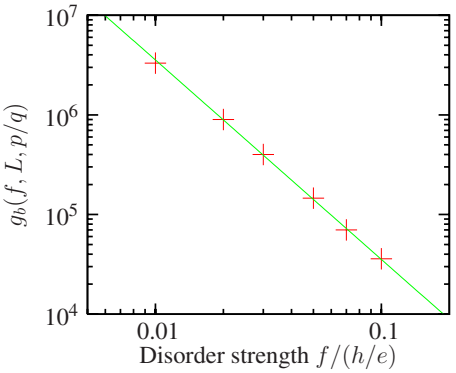

FIG. 8. (Color online) The disorder dependence of the fitting parameter $g_b(f,L,p/q)$. The size of the square samples is $L/a=128$ and the constant magnetic-flux density $B=1/32(h/e)a^{-2}$. From the log-log plot, a power-law relation $g_b(f,L,p/q)=355\times[f/(h/e)]^{-2}$ is obtained.

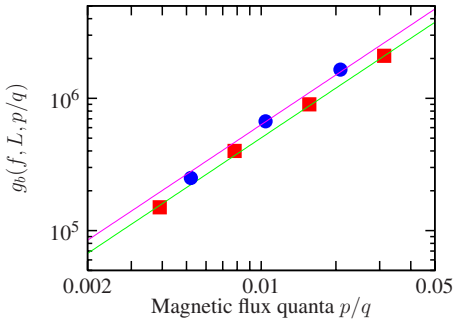

FIG. 9. (Color online) The power-law dependence of the fitting parameter $g_b(f,L,p/q)$ versus magnetic-flux quanta p/q for square samples of size $L/a=192$ (●) with $f/(h/e)=0.02$ and for $L/a=256$ with disorder strength $f/(h/e)=0.03$. The straight lines follow a $\propto(p/q)^{1.25}$ relation.

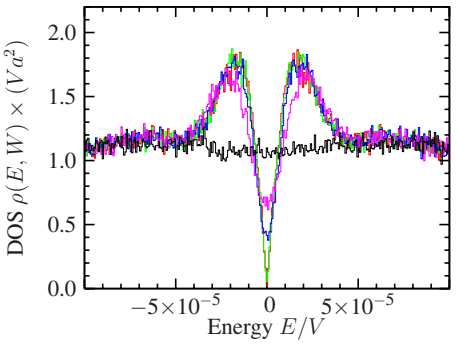

FIG. 10. (Color online) The disappearance of the depression in the density of states near the Dirac point due to an additional diagonal disorder potential of strength $W/V=10^{-5}$, 10^{-4}, 10^{-3}, 2×10^{-3}, and 10^{-2}, respectively. The system size is $L/a=128$, the random-flux disorder $f/(h/e)=0.05$, and the constant magnetic-flux density $B=1/32(h/e)a^{-2}$.

of the Landau band vary. In any case, the DOS tails become steeper with increasing B. For square samples of size $L/a=256$ and disorder strength $f/(h/e)=0.03$, a power-law relation $g_b(f,L,p/q)\propto(1/q)^{1.25}$ is extracted from a fit to the relation corresponding to Eq. (4) with $q=32$, 64, 128, and 256. A similar behavior is observed for $L/a=192$, $f/(h/e)=0.02$, and flux densities with $q=48$, 96, and 192. Both data fits can be seen in Fig. 9 on a double logarithmic scale. This magnetic field dependence means that the energy range of the DOS depression becomes broader and therefore more important when the magnetic-flux density gets smaller, approaching those applied in experiments. However, this power-law relation will probably only hold as long as the magnetic length $l_B=\sqrt{\hbar/(eB)}=a\sqrt{q/(2\pi p)}$ remains smaller than the system size L.

The size dependence of $g_b(f=0.01h/e,L,p/q=1/32)$ is found to be $\propto L^{2.5}$ in the range $64\leq L/a\leq192$. Although the tails of the DOS depression get steeper with increasing system size, $\rho(E/V=0)$ stays zero at the Dirac point in the range $64\leq L\leq512$ investigated. Putting everything together, in the presence of a perpendicular magnetic field the dependence of the empirical fitting function on disorder strength, system size, and magnetic-flux density can be summarized by $g_b\propto f^{-2}(L/l_B)^{5/2}$.

IV. DISCUSSION AND CONCLUSIONS

The density of states of noninteracting electrons moving on a two-dimensional bricklayer lattice in the presence of chiral symmetry preserving random-flux disorder and a perpendicular magnetic field exhibits a narrow depression near the Dirac point at $E/V=0$. The corresponding numerical results reveal a dependence on the disorder strength, the magnetic flux density, and on the size of the system. The latter is not simply a finite-size effect because the special size dependence develops only near the Dirac point where $\rho(E/V=0)$ stays zero even though the steepness of the tails grows with increasing L.

Since the DOS depression can be removed by an additional diagonal disorder giving rise to intervalley scattering, the origin of this feature must derive from the sublattice structure and the associated chiral symmetry of graphene's honeycomb lattice. The modeling of diagonal disorder required an extra term $\Sigma_{x,y}\epsilon_{x,y}c^{\dagger}_{x,y}c_{x,y}$ in the Hamiltonian (1). The set of uncorrelated random-disorder potentials $\{\epsilon_{x,y}\}$ was chosen to be box distributed $-W/2\leq\epsilon_{x,y}\leq W/2$ with probability density $1/W$. The removal of the DOS depression as a function of additional short-range disorder potentials can be seen in Fig. 10 for systems of size $L/a=128$, random-flux disorder $f/(h/e)=0.05$, and magnetic-flux density $B=1/32(h/e)a^{-2}$. With increasing disorder strength $W/V=10^{-5}$, 10^{-4}, 10^{-3}, 2×10^{-3}, and 10^{-2}, the narrow DOS depression in the lowest (central) Landau band completely disappears.

The occurrence of the DOS depression in the absence of short-range diagonal disorder for $B=0$ could be explained if the elastic-scattering length diverged at the Dirac point. Then, for increasing system size a decreasing energy range around $E/V=0$ would exist where the elastic-scattering length is larger than L. Within this energy interval, the transport would be almost ballistic and, due to the absence of scattering events, the DOS approaches the result of the ordered case and drops to zero at $E/V=0$. If this size dependence of the DOS depression were accessible in experiments, it would open the possibility for obtaining information about the elastic-scattering length.

Due to the lack of an analytical theory for the density of states of a disordered bricklayer model near the Dirac point, a relation proposed in the context of the thermal quantum-Hall effect[44,45] and recently for disordered Dirac fermions on a honeycomb lattice[24] was ventured. While the empirical relation, Eq. (4), used to fit the numerical results seems to work quite well, one has to keep in mind that only analytical calculations for a lattice model in the presence of random-magnetic flux will eventually help to understand the complete situation. The usual way to start from the continuum Dirac equation may turn out to be not appropriate for a comprehensive description, if the depression in the density of states found in the present study would not show up in the former description.

The implication of this observation and its impact on the scaling behavior and the critical properties at the Dirac point is evident but still needs to be investigated. Usually, a non-

critical density of states with a smooth energy dependence is assumed in the scaling analysis. In particular, the strong energy and size dependence reported above necessitate a reassessment of the conventional procedure applied in Ref. 18.

Although the disorder and magnetic field-dependent depression found in the density of states at the Dirac point and the occurrence of the conductance peak splitting reported previously[18] are in agreement with several aspects observed in experiments mentioned in the introduction, it is clear that many-body effects and also single-particle interactions such as Zeeman splitting or spin-orbit scattering, which were not taken into account in the present investigations, may turn out to be the dominant effects in understanding these experiments. Nevertheless, the results of the calculations presented above may be helpful in finding out which type of disorder determines the electronic properties of real graphene samples.

ACKNOWLEDGMENTS

I would like to thank Walter Apel, Ferdinand Evers, and Peter Markoš for helpful discussions.

[1] T. Ando, T. Nakanishi, and R. Saito, J. Phys. Soc. Jpn. **67**, 2857 (1998).
[2] M. I. Katsnelson, K. S. Novoselov, and A. K. Geim, Nat. Phys. **2**, 620 (2006).
[3] C. W. J. Beenakker, Rev. Mod. Phys. **80**, 1337 (2008).
[4] J. H. Bardarson, M. Titov, and P. W. Brouwer, Phys. Rev. Lett. **102**, 226803 (2009).
[5] T. Ando, Physica E (Amsterdam) **40**, 213 (2007).
[6] A. F. Young and P. Kim, Nat. Phys. **5**, 222 (2009).
[7] N. Stander, B. Huard, and D. Goldhaber-Gordon, Phys. Rev. Lett. **102**, 026807 (2009).
[8] Y. Hasegawa, Y. Hatsugai, M. Kohmoto, and G. Montambaux, Phys. Rev. B **41**, 9174 (1990).
[9] K. Wakabayashi, M. Fujita, H. Ajiki, and M. Sigrist, Phys. Rev. B **59**, 8271 (1999).
[10] Y. Hatsugai, T. Fukui, and H. Aoki, Phys. Rev. B **74**, 205414 (2006).
[11] K. S. Novoselov, A. Geim, S. V. Mozorov, D. Jiang, M. I. Katsnelson, I. V. Grigorieva, S. V. Dubonos, and A. A. Firsov, Nature (London) **438**, 197 (2005).
[12] Y. Zhang, Y.-W. Tan, H. L. Stormer, and P. Kim, Nature (London) **438**, 201 (2005).
[13] A. J. M. Giesbers, U. Zeitler, M. I. Katsnelson, L. A. Ponomarenko, T. M. Mohiuddin, and J. C. Maan, Phys. Rev. Lett. **99**, 206803 (2007).
[14] Y.-W. Tan, Y. Zhang, K. Bolotin, Y. Zhao, S. Adam, E. H. Hwang, S. Das Sarma, H. L. Stormer, and P. Kim, Phys. Rev. Lett. **99**, 246803 (2007).
[15] P. M. Ostrovsky, I. V. Gornyi, and A. D. Mirlin, Phys. Rev. B **74**, 235443 (2006).
[16] M. Koshino and T. Ando, Phys. Rev. B **75**, 033412 (2007).
[17] P. M. Ostrovsky, I. V. Gornyi, and A. D. Mirlin, Phys. Rev. B **77**, 195430 (2008).
[18] L. Schweitzer and P. Markoš, Phys. Rev. B **78**, 205419 (2008).
[19] K. Nomura and A. H. MacDonald, Phys. Rev. Lett. **98**, 076602 (2007).
[20] D. N. Sheng, L. Sheng, and Z. Y. Weng, Phys. Rev. B **73**, 233406 (2006).
[21] T. Kawarabayashi, Y. Hatsugai, and H. Aoki, Phys. Rev. Lett. **103**, 156804 (2009).
[22] I. L. Aleiner and K. B. Efetov, Phys. Rev. Lett. **97**, 236801 (2006).
[23] A. Altland, Phys. Rev. Lett. **97**, 236802 (2006).
[24] B. Dóra, K. Ziegler, and P. Thalmeier, Phys. Rev. B **77**, 115422 (2008).
[25] A. W. W. Ludwig, M. P. A. Fisher, R. Shankar, and G. Grinstein, Phys. Rev. B **50**, 7526 (1994).
[26] A. A. Nersesyan, A. M. Tsvelik, and F. Wenger, Phys. Rev. Lett. **72**, 2628 (1994).
[27] W. A. Atkinson, P. J. Hirschfeld, A. H. MacDonald, and K. Ziegler, Phys. Rev. Lett. **85**, 3926 (2000).
[28] D. V. Khveshchenko, EPL **82**, 57008 (2008).
[29] N. M. R. Peres, F. Guinea, and A. H. Castro Neto, Phys. Rev. B **73**, 125411 (2006).
[30] S. Wu, L. Jing, Q. Li, Q. W. Shi, J. Chen, H. Su, X. Wang, and J. Yang, Phys. Rev. B **77**, 195411 (2008).
[31] V. M. Pereira, J. M. B. Lopes dos Santos, and A. H. Castro Neto, Phys. Rev. B **77**, 115109 (2008).
[32] B. Hu, E. H. Hwang, and S. Das Sarma, Phys. Rev. B **78**, 165411 (2008).
[33] K. Ziegler, B. Dóra, and P. Thalmeier, Phys. Rev. B **79**, 235431 (2009).
[34] S. Ryu and Y. Hatsugai, Phys. Rev. B **65**, 033301 (2001).
[35] Y. Zhang, Z. Jiang, J. P. Small, M. S. Purewal, Y.-W. Tan, M. Fazlollahi, J. D. Chudow, J. A. Jaszczak, H. L. Stormer, and P. Kim, Phys. Rev. Lett. **96**, 136806 (2006).
[36] Z. Jiang, Y. Zhang, H. L. Stormer, and P. Kim, Phys. Rev. Lett. **99**, 106802 (2007).
[37] A. J. M. Giesbers, L. A. Ponomarenko, K. S. Novoselov, A. K. Geim, M. I. Katsnelson, J. C. Maan, and U. Zeitler, Phys. Rev. B **80**, 201403 (2009).
[38] J. G. Checkelsky, L. Li, and N. P. Ong, Phys. Rev. Lett. **100**, 206801 (2008).
[39] J. G. Checkelsky, L. Li, and N. P. Ong, Phys. Rev. B **79**, 115434 (2009).
[40] S. V. Morozov, K. S. Novoselov, M. I. Katsnelson, F. Schedin, L. A. Ponomarenko, D. Jiang, and A. K. Geim, Phys. Rev. Lett. **97**, 016801 (2006).
[41] F. Guinea, M. I. Katsnelson, and M. A. H. Vozmediano, Phys. Rev. B **77**, 075422 (2008).
[42] M. I. Katsnelson and A. K. Geim, Philos. Trans. R. Soc. London, Ser. A **366**, 195 (2008).
[43] Y. Morita and Y. Hatsugai, Phys. Rev. Lett. **79**, 3728 (1997).
[44] A. Mildenberger, F. Evers, A. D. Mirlin, and J. T. Chalker, Phys. Rev. B **75**, 245321 (2007).
[45] F. Evers and A. D. Mirlin, Rev. Mod. Phys. **80**, 1355 (2008).
[46] Y. Zheng and T. Ando, Phys. Rev. B **65**, 245420 (2002).